



Radiation synthesis of ionic liquid–functionalized silica-based adsorbents: a preliminary investigation on its application for removal of ReO_4^- as an analog for TcO_4^-

Kangjun Xie^{1,2} · Zhen Dong¹ · Long Zhao¹

Received: 1 October 2020 / Accepted: 13 December 2020 / Published online: 5 January 2021

© The Author(s), under exclusive licence to Springer-Verlag GmbH, DE part of Springer Nature 2021

Abstract

The decontamination of radioactive TcO_4^- from nuclear wastes is becoming increasingly crucial for spent nuclear fuel reprocessing and environmental remediation. In this work, a series of ionic liquid–immobilized silica-based adsorbents (SVIL-C_n, $n = 1, 4, 8$) were newly synthesized using the radiation-induced grafting of 4-vinylbenzyl chloride onto silanized silica and subsequent functionalization with 1-methylimidazole, 1-butylimidazole, or 1-octylimidazole. The synthesis conditions such as the solvent, absorbed dose, and monomer concentration were investigated in detail, and the resulting adsorbents were characterized by elemental analysis, FT-IR, SEM, and TGA. In batch experiments, the adsorbents exhibited a high ReO_4^- (a non-radioactive surrogate of TcO_4^-) removal efficiency over a wide pH range (3 ~ 8), and SVIL-C1 showed a maximum adsorption capacity of 70.62 mg g⁻¹ towards ReO_4^- . In addition, their adsorption performance barely changed after 800 kGy radiation. The column experiments for treating simulated radioactive wastewater showed that the SVIL-C_n adsorbents could selectively separate $\text{TcO}_4^-/\text{ReO}_4^-$ from a variety of fission products, and they could be recycled four times with negligible capacity loss. Lastly, XPS and FT-IR analysis confirmed that the adsorption proceeded via an ion-exchange mechanism. The results showed that these adsorbents are suitable for the efficient removal of $\text{TcO}_4^-/\text{ReO}_4^-$ from radioactive wastewater with complex compositions.

Keywords Silica · Ionic liquid · Radiation grafting · ReO_4^- · TcO_4^-

Responsible Editor: Tito Roberto Cadaval Jr

Highlights

- Ionic liquid–modified silica adsorbents were newly synthesized by radiation grafting.
- The prepared adsorbents could selectively remove ReO_4^- from simulated radioactive waste.
- The adsorbents could be recycled four times with negligible capacity loss.
- The adsorption performance barely changed after 800 kGy radiation.

✉ Long Zhao
ryuuchou@hotmail.com; zhaolong@hust.edu.cn

¹ State Key Laboratory of Advanced Electromagnetic Engineering and Technology, School of Electrical and Electronic Engineering, Huazhong University of Science and Technology, Wuhan 430074, China

² School of Chemistry and Chemical Engineering, Huazhong University of Science and Technology, Wuhan 430074, China

Introduction

Technetium-99 (⁹⁹Tc) is one of the most important radionuclides in nuclear waste treatment because of its long half-life ($t_{1/2} = 2.13 \times 10^5$ years), high fission yield (6.03%), and high mobility (Lee et al. 2016; Shi et al. 2012). ⁹⁹Tc primarily exists in its most stable oxidation state of TcO_4^- , which is difficult to immobilize during nuclear waste disposal (Yu et al. 2010). Thus, due to its high solubility and mobility, TcO_4^- is more likely to diffuse into the environment and causes more severe pollution than other radionuclides. A large fraction of TcO_4^- also evaporates from the smelter into off-gas equipment, causing hidden safety issues during the vitrification of radioactive waste (Liu and Han 2019); therefore, it is important to develop a strategy to efficiently capture TcO_4^- from radioactive wastewater.

Adsorption is one of the most promising techniques for capturing TcO_4^- because of its low cost, facile operation, and high efficiency (Dong et al. 2016). A variety of materials have been used to remove TcO_4^- , such as activated carbons

(Galamboš et al. 2015), natural polymers (Wang et al. 2021), synthetic resins (Zu et al. 2016b), and clay minerals (Yang et al. 2019). Some new adsorbents such as metal-organic frameworks (MOFs) (Sheng et al. 2017, 2019) and covalent organic frameworks (COFs) (Lin et al. 2017; Wang et al. 2020) have been recently developed to decontaminate TcO_4^- , but these materials have some shortcomings in practical applications because of the properties of radioactive wastewater. For example, clay minerals and activated carbons are cheap and easy to obtain, but they have a poor selectivity and adsorption capacity. Traditional polymer resins efficiently remove TcO_4^- but have weak radiation resistance. The high cost, complicated synthesis, difficulty in column packing, and poor cyclic stability of MOFs and COFs restrict their applications in practical large-scale treatment methods (Yang et al. 2019). Therefore, there is an urgent need to develop a novel material that can be employed for radioactive wastewater that is low-cost, radiation-resistant, efficient, and suitable for large-scale applications.

Silica is a widely used adsorbent substrate because of its excellent chemical, thermal, and radiation stability and controllable structure, which make it an ideal adsorbent substrate for treating radioactive wastewater (Morin-Crini et al. 2018). Previously, a series of functional monomers was grafted onto silica to absorb nonradioactive metal ions and radionuclides (Chen et al. 2017). Ionic liquids are green functional monomers with good chemical and thermal stability, radiation resistance, and tunable properties, and they have been extensively applied for extraction separation (Favre-Réguillon et al. 2019; Pepper and Ogden 2013; Zsabka et al. 2019). Ionic liquids immobilized on solid substrates have also shown better separation performance than free ionic liquids (Dong and Zhao 2018; Zhao et al. 2016); therefore, it is expected that adsorbents with excellent radiation stability and adsorption properties can be obtained by immobilizing ionic liquid onto silica. In recent years, ionic liquids have been immobilized onto silica for adsorption separation using traditional chemical methods (Qian et al. 2016; Mahmoud and Al-Bishri 2011); however, considering the low chemical reactivity between ionic liquids and silica, there is a need to develop a more efficient strategy for immobilizing ionic liquids onto silica.

Radiation grafting is an efficient chemical modification method because no catalysts or additives are required, and the grafting reaction can be easily adjusted by varying the radiation conditions (Xie et al. 2019; Dong et al. 2019). Some organic functional monomers such as dimethylaminoethyl methacrylate (Zhao et al. 2011) and acrylamide (Xu et al. 2011) have been grafted onto silica using a radiation technique, but there are few reports about the radiation grafting of ionic liquids.

In this work, to develop cost-effective adsorbents with good radiation stability and adsorption properties, a series of imidazolium ionic liquids functionalized micron-sized silica adsorbents were synthesized by the radiation grafting of 4-vinylbenzyl chloride (VBC) onto silanized silica, followed

by modification using a series of imidazole with different alkyl chains. Due to the radioactivity of TcO_4^- , the separation of TcO_4^- cannot be carried out in a typical laboratory; therefore, ReO_4^- , which has similar chemical properties and ionic radius to TcO_4^- , is often widely studied as a TcO_4^- analog (Banerjee et al. 2016). In addition, rhenium (Re) is one of the rarest metallic elements on the earth, and it has been widely used in many fields (Zu et al. 2016a). Therefore, the adsorption of ReO_4^- by the prepared adsorbents (SVIL-Cn) was studied via batch and column experiments, and the radiation resistance and adsorption mechanism were studied.

Materials and methods

Materials

Column-layer chromatographic silica gel (SiO_2 , purity: 98%, type: C116881) with diameter of 120–150 μm was purchased from Aladdin Chemical Co., Ltd. Methacryloxy propyl trimethoxyl silane (MPTS), 1-methylimidazole, 1-butylimidazole, 1-octylimidazole, and 4-vinylbenzyl chloride (VBC) were obtained from Aladdin Chemical Co., Ltd. Potassium perrhenate and Triton X-100 were obtained from Macklin Chemical Co., Ltd. Re standard solution was provided by NCS Testing Technology Co., Ltd. All chemicals were used as received without further purification. Ultrapure water was used during all experiments.

Synthesis of adsorbents

The SiO_2 was activated in 6 mol L^{-1} HCl for 24 h. Then, it was washed to neutral by ultrapure water and dried at 80 °C. Subsequently, 5 g activated SiO_2 , 5 mL MPTS, and 45 mL toluene were mixed into a teflon-lined stainless-steel reactor, and heated for 24 h at 120 °C. The silanized silica (denoted as SiO_2 -MPTS) was obtained after removing unreacted MPTS by washing with ethanol and ultrapure water and dried at 60 °C.

About 1 g SiO_2 -MPTS was vacuum-sealed in a polyethylene bag. Then, deoxygenated 10 mL 4-vinylbenzyl chloride solution was injected into a polyethylene bag. The samples were irradiated at room temperature with the dose rate of 20 kGy/pass by electron beam accelerator (Wasik Associates INC, USA) at 1 MeV. Subsequently, the homopolymers and unreacted monomers were removed by ethanol and ultrapure water. The SiO_2 -MPTS-VBC was obtained after drying at 60 °C. The grafting yield (GY) was calculated using Eq. (1),

$$\text{GY} = \frac{W_g - W_0}{W_0} \times 100\% \quad (1)$$

where W_0 (g) and W_g (g) were the weight of SiO_2 -MPTS and SiO_2 -MPTS-VBC, respectively.

Finally, 1 g SiO₂-MPTS-VBC, 2 mL 1-methylimidazole, and 18 mL toluene were mixed into the teflon-lined stainless-steel reactor, and heated for 24 h at 120 °C. The SVIL-C1 was obtained after washing with ethanol and ultrapure water and dried. The SVIL-C4 and SVIL-C8 were synthesized in the same way using 1-butylimidazole and 1-octylimidazole, respectively. The synthesis route of SVIL-Cn (*n* = 1, 4, 8) is shown in Fig. 1. The SVIL-Cn contained ionic liquids composed of the alkylimidazolium cation and chloride anion and were used for removal of ReO₄[−].

Characterization of adsorbents

Fourier transform infrared spectrometry (FT-IR) was done using a spectrophotometer (Bruker Tensor 27) in the wavenumber range of 4000–450 cm^{−1}. Thermogravimetric analysis (TGA) curves were recorded on a TGA 55 (TA instruments) in a temperature range of room temperature to 800 °C at a heating rate of 10 °C min^{−1} with the oxygen atmosphere. The surface morphology was investigated by using a scanning electron microscope (SEM) (Hitachi SU8000, Japan). The X-ray photoelectron spectroscopy (XPS) spectra were recorded by an AXIS-Ultra DLD instrument (SHIMADZU, Japan) and fitted with the XPSPEAK4.1 software. The element composition of prepared adsorbents was investigated by using a Vario Micro cube (Elementar, Germany). The N₂ adsorption/desorption measurements were performed on the ASAP2420-4MP (Micromeritics USA). The concentrations of ReO₄[−] and coexisting cations were determined by using an inductively coupled plasma atomic emission spectrometer (ICP-OES 5110, Agilent, USA). The concentration of Cl[−] was determined by ion chromatography (Metrohm, Switzerland)

Batch adsorption experiments

The batch adsorption experiments were carried out through mixing 10 mg adsorbent and 10 mL KReO₄ solution in a glass bottle and shaken at a speed of 160 rpm for a certain time. Then the supernatant was separated using the filter with a pore size of 450 nm. The concentrations of ReO₄[−] before and after adsorption were determined by ICP-OES. The effect of pH,

contact time, initial concentration, temperature, and coexisting ions on the removal efficiency of ReO₄[−] onto SVIL-Cn were studied with a similar procedure. The adsorption capacity (*q_e*, mg g^{−1}) and adsorption efficiency (*E*, %) were calculated by using Eq. (2) and Eq. (3), respectively.

$$q_e = \frac{(c_0 - c_e)V}{m} \quad (2)$$

$$E = \frac{(c_0 - c_e)}{c_0} \times 100\% \quad (3)$$

where *c*₀ (ppm) and *c_e* (ppm) are the initial concentration and equilibrium concentration, respectively. *V* (mL) and *m* (mg) are the volume of the solution and the mass of adsorbent, respectively.

Column adsorption experiments

About 1 g adsorbent was placed into the polypropylene column with a dimension of 5 × 60 mm. The simulated radioactive wastewater (SRW) which contained 0.1 mmol L^{−1} Re (VII), Ce(III), Cs(I), Eu(III), La(III), Nd(III), Sc(III), and 0.5 mol L^{−1} HNO₃ was pumped by using a peristaltic pump through the column at a certain flow rate. A certain amount of SRW, deionized water, 3 mol L^{−1} HNO₃, and deionized water flowed through the column in turn and cycled four times. The concentration of ReO₄[−] and coexisting cations in the outflow were determined by ICP-OES.

Radiation stability experiments

In order to investigate the radiation resistance of adsorbents, a 0.1 g adsorbent was sealed in a polyethylene bag and then irradiated using β-rays (1 MeV accelerator) and γ-rays (⁶⁰Co source) with different doses of 200, 400, and 800 kGy. The adsorption performance and FT-IR spectra of adsorbents after radiation were studied. The adsorption experiments of irradiated adsorbents were carried out according to the “Batch adsorption experiments” section.

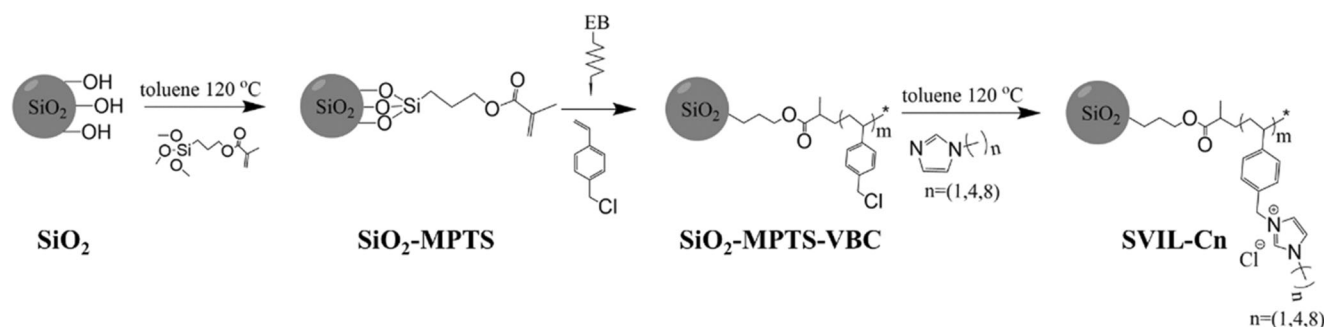


Fig. 1 Synthesis route of SVIL-Cn

Results and discussion

Preparation of SVIL-Cn

The prepared SiO₂-MPTS formed white amorphous particles with an average size of 180 μm with a MPTS content of about 20 wt%. Then, VBC was grafted onto SiO₂-MPTS using a simultaneous irradiation technique. VBC is a hydrophobic monomer, and the grafting reaction of VBC is usually carried out in organic solvents such as methanol or toluene (Wang et al. 2021; Herman et al. 2003). Ting et al. found that methanol enhanced the VBC diffusion to grafting sites at a rate higher than other alcohols with different alkyl chains (Ting et al. 2015). Several studies have also suggested that the GY of hydrophobic monomers is greater in an emulsion than in an organic solvent-mediated grafting system (Ting and Nasef 2017); therefore, methanol and emulsion systems were selected for the radiation grafting of VBC. The effect of solvent on GY is shown in Fig. 2a. The GY in the Triton X-100/H₂O emulsion system was higher than that obtained in methanol, mainly because there were more monomer molecules in the micelles, which effectively supplied monomer to the grafting zone (Ting and Nasef 2017). Therefore, an emulsion system was applied to the subsequent grafting reaction. From Fig. 2b, it can be found that GY increased upon increasing the absorbed dose and gradually tended to equilibrium. This was because the radiation graft polymerization proceeded via a free-radical mechanism, and upon increasing the absorbed dose, more free radicals and reactive sites were generated on SiO₂-MPTS, which accelerated the grafting reaction. As the absorbed dose continued to increase, GY tended to equilibrium because of accelerated side reactions such as cross-linking and chain-transfer at higher doses. The illustration in Fig. 2b shows that GY increased first and then decreased upon increasing the monomer concentration, mainly because more monomers

diffused to reactive sites for the grafting reaction. Further increasing the monomer concentration increased the viscosity of the grafting system, which inhibited monomer diffusion (Ting et al. 2015). The maximum grafting yield was 36.05% at an absorbed dose of 160 kGy and monomer concentration of 20 wt%; therefore, this radiation grafting condition was selected to synthesize SiO₂-MPTS-VBC. Subsequently, SVIL-C1, SVIL-C4, and SVIL-C8 were synthesized by nucleophilic substitution between SiO₂-MPTS-VBC and 1-methylimidazole, 1-butylimidazole, and 1-octylimidazole, respectively.

Characterization

The structure and morphology of the adsorbents were characterized by FT-IR, XPS, TGA, SEM, and elemental analysis. As shown in Fig. 3a, the peaks at 1726 cm⁻¹ and 2800–3050 cm⁻¹ were assigned to the absorption of C=O and C–H group in MPTS (Xiao et al. 2016), which confirmed the successful synthesis of SiO₂-MPTS. The successful grafting of VBC was verified by the appearance of a new peak at 678 cm⁻¹ which was ascribed to the absorption of C–Cl bonds (Xu et al. 2010). The characteristic peak of the imidazole ring at 1570 cm⁻¹ demonstrated the successful introduction of imidazole (Feng et al. 2016).

The XPS spectra of SiO₂, SiO₂-MPTS, SiO₂-MPTS-VBC, and SVIL-C1 are shown in Fig. 3b. The SiO₂ spectrum contains peaks of O 1s, Si 2s, and Si 2p. The new C 1s peak in the SiO₂-MPTS spectrum suggested that SiO₂ was successfully silanized. After the radiation grafting of VBC, the Cl 2s and Cl 2p peaks appeared, which indicated that VBC was successfully grafted onto silanized silica. Finally, a new N 1s peak indicated that SVIL-C1 was successfully synthesized.

The TGA and DTG curves in Fig. 3c and d show that the thermal degradation of SiO₂, SiO₂-MPTS, SiO₂-MPTS-VBC, and SVIL-Cn were one-step, two-step, three-step, and four-

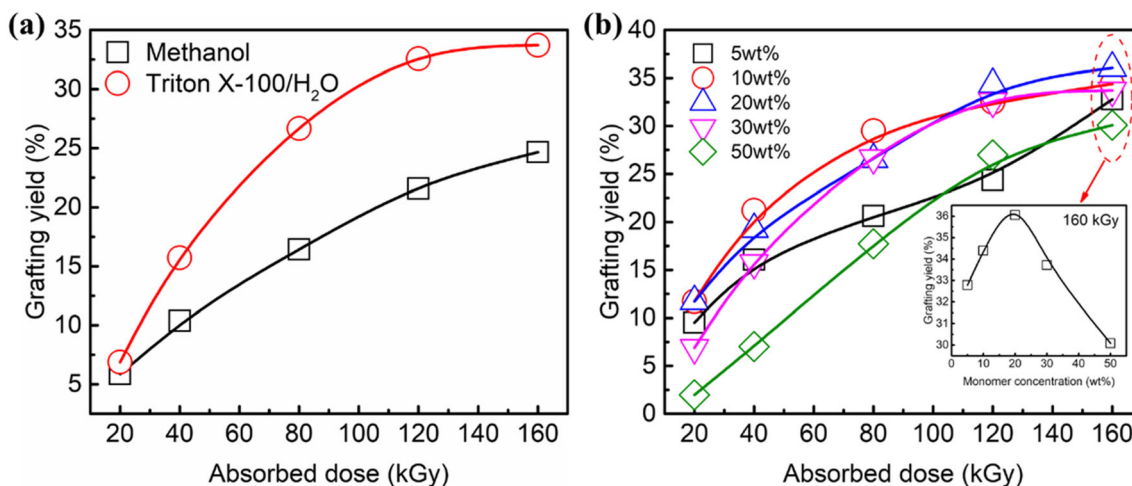


Fig. 2 a Effect of solvent on GY of SiO₂-MPTS-VBC (monomer concentration of 30 wt%). b Effect of monomer concentration on GY of SiO₂-MPTS-VBC in the emulsion system

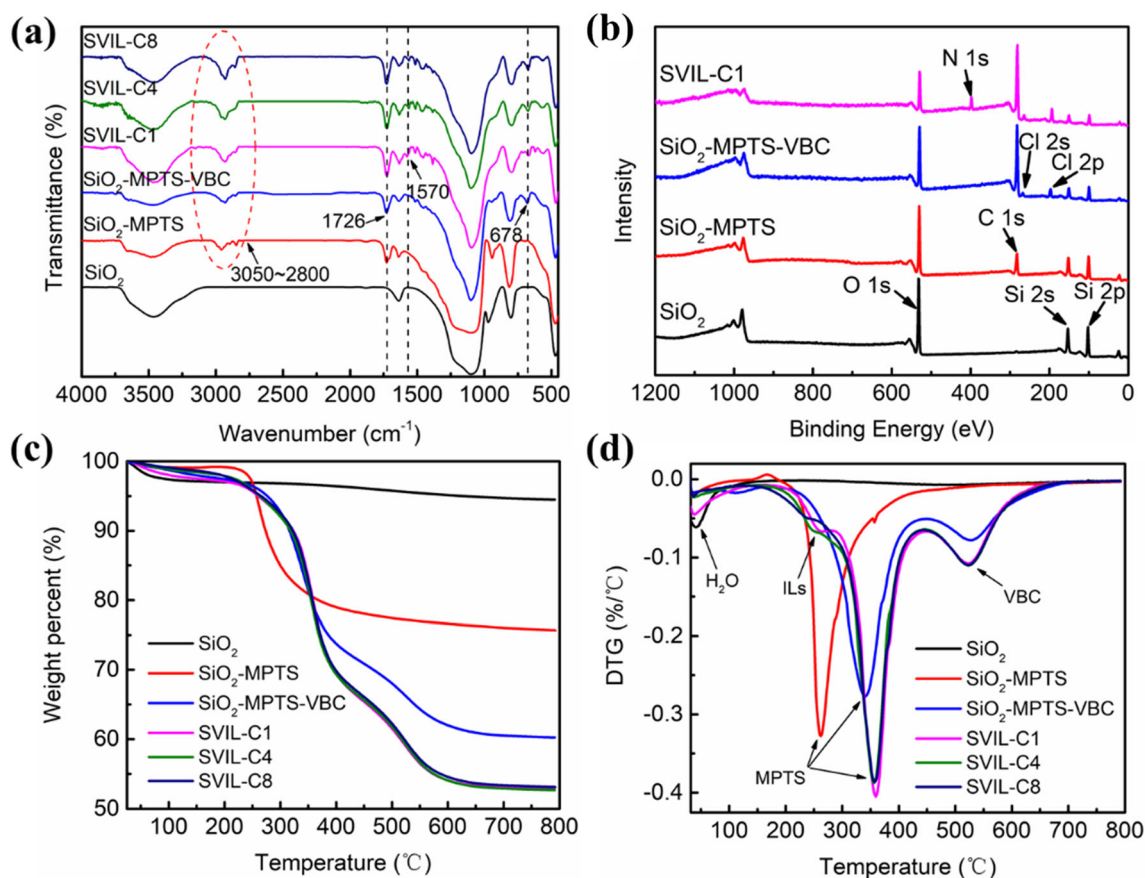


Fig. 3 FT-IR (a), XPS (b), TGA (c), and DTG (d) spectra of SiO_2 , SiO_2 -MPTS, SiO_2 -MPTS-VBC, and SVIL-C $_n$ ($n = 1, 4, 8$)

step processes, respectively. The thermal degradation of SiO_2 involved only one step from room temperature to 100 °C, which was considered to be the loss of physically adsorbed water (Zhao et al. 2011). For SiO_2 -MPTS, the weight-loss stage from 250 to 400 °C was due to the degradation of MPTS (Xiao et al. 2016). The weight loss of SiO_2 -MPTS-VBC between 450 and 650 °C was attributed to the degradation of grafted VBC. The weight loss of ILs in SVIL-C $_n$ occurred from 200 to 300 °C. The TGA curves confirm that SVIL-C $_n$ was successfully synthesized and was stable below 200 °C.

Figure 4 shows the SEM images of SiO_2 , SiO_2 -MPTS, SiO_2 -MPTS-VBC, and SVIL-C1. The original SiO_2 was smooth amorphous particles with no bulges or cracks and a particle size of about 150 μm . After silanization and grafting, the surface became rough, and the particle size slightly increased, indicating that SiO_2 was successfully modified.

The elemental analysis and N_2 adsorption/desorption isotherms of the three adsorbents are shown in Table 1. The amount of N indicated how many imidazolium groups were functionalized on the surface of SiO_2 -MPTS-VBC. The elemental analysis results showed that the imidazolium molar content of SVIL-C $_n$ decreased upon increasing the alkyl chain length. Compared with SiO_2 -MPTS-VBC, the specific surface areas and pore volumes of all three adsorbents were lower. The imidazolium molar content of SVIL-C8 was the lowest,

but its specific surface area and pore volume showed the greatest decrease, which indicated that longer alkyl chains occupied more pore volume. The above characterization results demonstrate the successful synthesis of SVIL-C $_n$.

Batch adsorption experiments

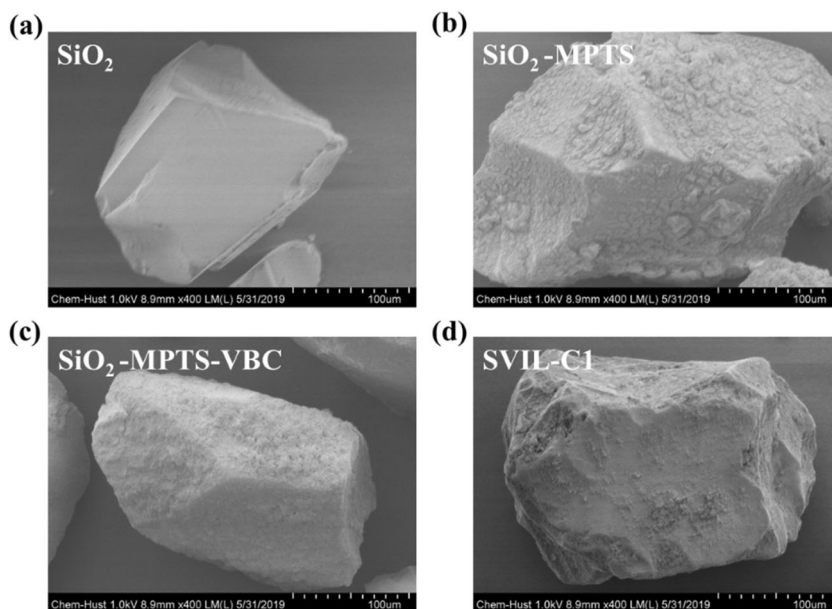
Influence of pH

The influence of pH on the ReO_4^- adsorption was investigated at different initial pH values from 1 to 8. As shown in Fig. 5a, the removal efficiency of ReO_4^- was unaffected by the pH value over a wide range from 3 to 8. The removal efficiency decreased when the pH was lower than 3, mainly because Cl^- influenced the adsorption of ReO_4^- by participating in an anion exchange (Lou et al. 2019). The adsorption trends of these three adsorbents at different pH values were not significantly different; thus, a natural pH was chosen for further adsorption experiments.

Adsorption kinetics, adsorption isotherms, and thermodynamics

In order to ensure a sufficient contact time to reach ReO_4^- adsorption equilibrium, the effect of contact time on the removal efficiency of ReO_4^- by SVIL-C $_n$ was studied. As

Fig. 4 SEM images of SiO₂ (a), SiO₂-MPTS (b), SiO₂-MPTS-VBC (c), and SVIL-C1 (d)



shown in Fig. 5b, all three adsorbents exhibited fast adsorption kinetics, mainly because the functional groups of adsorbents synthesized using radiation grafting were distributed on the substrate surface. SVIL-C1 showed the fastest adsorption rate, and it reached adsorption equilibrium in 60 min, mainly because it was more hydrophilic than SVIL-C4 and SVIL-C8, which facilitated the diffusion of ReO₄⁻ to the adsorption sites. In addition, the pseudo-first-order and pseudo-second-order models were applied to fit the adsorption kinetics data, and the fitting results are shown in Table S1 and Fig. S1. The adsorbents showed a high coefficient of determination R² for the pseudo-second-order model, which indicated that the rate-determining step of the adsorption of ReO₄⁻ onto SVIL-Cn may be chemical adsorption.

The adsorption isotherms of adsorption of ReO₄⁻ by SVIL-Cn are shown in Fig. 5c. The experimental data were fitted by the Langmuir and Freundlich models, and the fitting results are shown in Fig. S2 and Table 2. The experimental data of these three adsorbents were all fitted well by the Langmuir model, which revealed that the adsorption process of ReO₄⁻ onto SVIL-Cn was mainly monolayer adsorption on a homogeneous surface. The experiment showed that the order of the maximum adsorption

capacity (q_m) was SVIL-C1 (70.62 mg g⁻¹) > SVIL-C4 (48.78 mg g⁻¹) > SVIL-C8 (30.57 mg g⁻¹). This was mainly due to the higher molar content of imidazolium (n_{im}) in SVIL-C1, which was calculated from the elemental analysis results. The q_m/n_{im} of ReO₄⁻ adsorbed on SVIL-Cn are shown in Table 2. SVIL-C4 exhibited the largest q_m/n_{im} value, which was similar to another research (Lou et al. 2019). This was mainly due to the hydrophobicity and steric hindrance of the adsorbents, where highly hydrophobic adsorbents with low steric hindrance possessed a greater affinity for ReO₄⁻ (Jie et al. 2018). The maximum adsorption capacity of SVIL-C1 is higher than that of some previously reported adsorbents, as shown in Table S2. MOFs and COFs have exhibited a higher adsorption capacity than SVIL-Cn, but the high cost, complicated synthesis, difficult column packing, and poor cyclic stability of these materials restrict their applications in practical large-scale treatment methods. Comparatively, the SVIL-Cn adsorbents have a lower cost and easier synthesis, and can be used in adsorption columns for large-scale applications. Compared with resins, the SVIL-Cn adsorbents have similar adsorption capacities and better radiation resistance, giving them better application prospects.

Table 1 The elemental analysis and N₂ adsorption/desorption measurement results of SiO₂-MPTS-VBC, SVIL-C1, SVIL-C4, and SVIL-C8

Adsorbent	N%	Imidazolium molar content (mmol g ⁻¹)	Specific surface area (m ² g ⁻¹)	Pore volume (mm ³ g ⁻¹)
SiO ₂ -MPTS-VBC	-	-	32.21	38.80
SVIL-C1	1.349	0.482	3.646	7.752
SVIL-C4	0.874	0.312	2.621	5.107
SVIL-C8	0.654	0.234	1.644	2.826

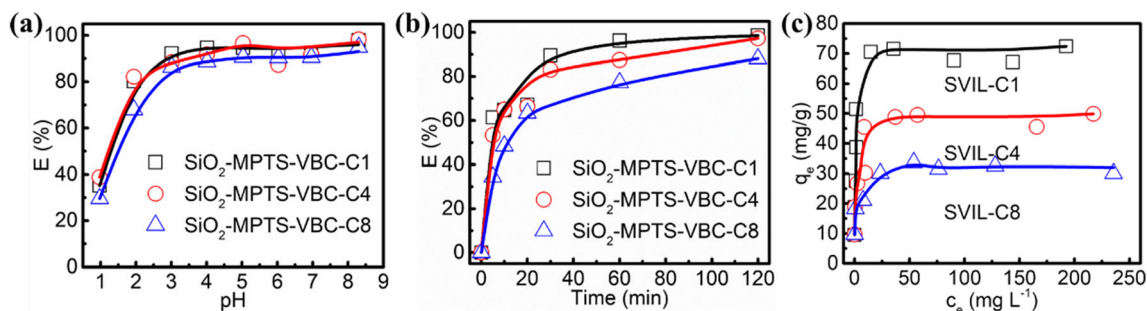


Fig. 5 a Effect of pH on the removal efficiency of ReO_4^- by SVIL-Cn ($c_0 = 20$ ppm). b Effect of contact time on the removal efficiency of ReO_4^- by SVIL-Cn ($c_0 = 20$ ppm, natural pH). c The adsorption isotherms of ReO_4^- onto SVIL-Cn (natural pH)

Competitive adsorption

Selectivity is a critical performance parameter for adsorbents because many ions coexist in radioactive wastewater. To investigate the selectivity of SVIL-Cn, some representative cations in radioactive wastewater including Eu(III), Sc(III), Cs(I), La(III), Ce(III), and Nd(III) were used for competitive adsorption experiments. As shown in Fig. 6, SVIL-Cn exhibited good selectivity with almost no adsorption of coexisting cations. The effect of coexisting anions (Cl^- , NO_3^- , SO_4^{2-} , PO_4^{3-}) on the removal efficiency of ReO_4^- onto SVIL-Cn was also investigated. The removal efficiency of ReO_4^- by SVIL-Cn decreased upon increasing the anion concentration, which was attributed to the competition for ion exchange sites between coexisting anions and ReO_4^- . The high concentration of NO_3^- showed the strongest interference for ReO_4^- adsorption among the anions, because of the similar ionic radius and same charge number of NO_3^- (0.67 nm) and ReO_4^- (0.70 nm) (Lou et al. 2019). The adsorption rate of ReO_4^- by SVIL-Cn remained at more than 50%, even when the coexisting anions were present in 100-fold excess, demonstrating the good selectivity of SVIL-Cn for ReO_4^- .

Radiation resistance

Radiation resistance is one of the most important properties of adsorbents used to treat radioactive wastewater, but many adsorbents based on polymeric materials have poor radiation resistance. To investigate the radiation resistance of SVIL-Cn, the adsorption performance and FT-IR spectra of SVIL-

Cn before and after radiation treatment were studied. As shown in Fig. 7 and Fig. S3, the removal efficiency and FT-IR spectra were almost unchanged after the materials were irradiated with extremely high doses (800 kGy) of β -rays and γ -rays. This is a very important advantage of SVIL-Cn over most commercial resins such as Purolite A532E and A530E (Jie et al. 2018).

Column experiments of simulated radioactive wastewater

To further evaluate the practical application prospects of SVIL-Cn, the column adsorption of ReO_4^- from simulated radioactive wastewater (SRW) was investigated using SVIL-C1 as the representative. As shown in Fig. 8, SVIL-C1 selectively separated ReO_4^- from SRW, while hardly adsorbing other compounds. The elution rate of ReO_4^- reached 100%, and the separation performance remained unchanged after three cycles. These results show that SVIL-C1 can selectively separate $\text{TcO}_4^-/\text{ReO}_4^-$ from radioactive wastewater.

Adsorption mechanism

To determine the adsorption mechanism, the FT-IR and XPS spectra of SVIL-C1 before and after capturing ReO_4^- were obtained. In the FT-IR spectra in Fig. 9a, a new peak at 905 cm^{-1} of ReO_4^- appeared after adsorption (Xingxiao et al. 2018). After desorption by $3\text{ mol L}^{-1}\text{ HNO}_3$, the ReO_4^- peak disappeared, and a new peak of NO_3^- at 1388 cm^{-1} indicating that ReO_4^- was replaced by NO_3^- after desorption. For the XPS spectra in Fig. 9b, the Cl peak disappeared, and a Re peak appeared after adsorption, which indicated that Cl^- was replaced by ReO_4^- . Figure 9c shows the Re 4f spectra of SVIL-C1 after adsorption. The peaks at binding energies of 48.45 and 46.08 eV were assigned to $4f_{5/2}$ and $4f_{7/2}$, respectively. This indicated that the Re species in SVIL-C1-Re existed as ReO_4^- , indicating the absence of a redox reaction during adsorption. As shown in Fig. 9d, the imidazolium N^+ peak shifted to a higher binding energy after adsorption, suggesting that there were strong interactions between the

Table 2 The q_m/n_{im} and parameters for Langmuir models of ReO_4^- adsorption on SVIL-Cn

Adsorbent	q_m (mg g^{-1})	R^2	n_{im} (mmol g^{-1})	q_m/n_{im} (mg mmol^{-1})
SVIL-C1	70.62	0.998	0.482	146.51
SVIL-C4	48.78	0.997	0.312	156.35
SVIL-C8	30.57	0.998	0.234	130.64

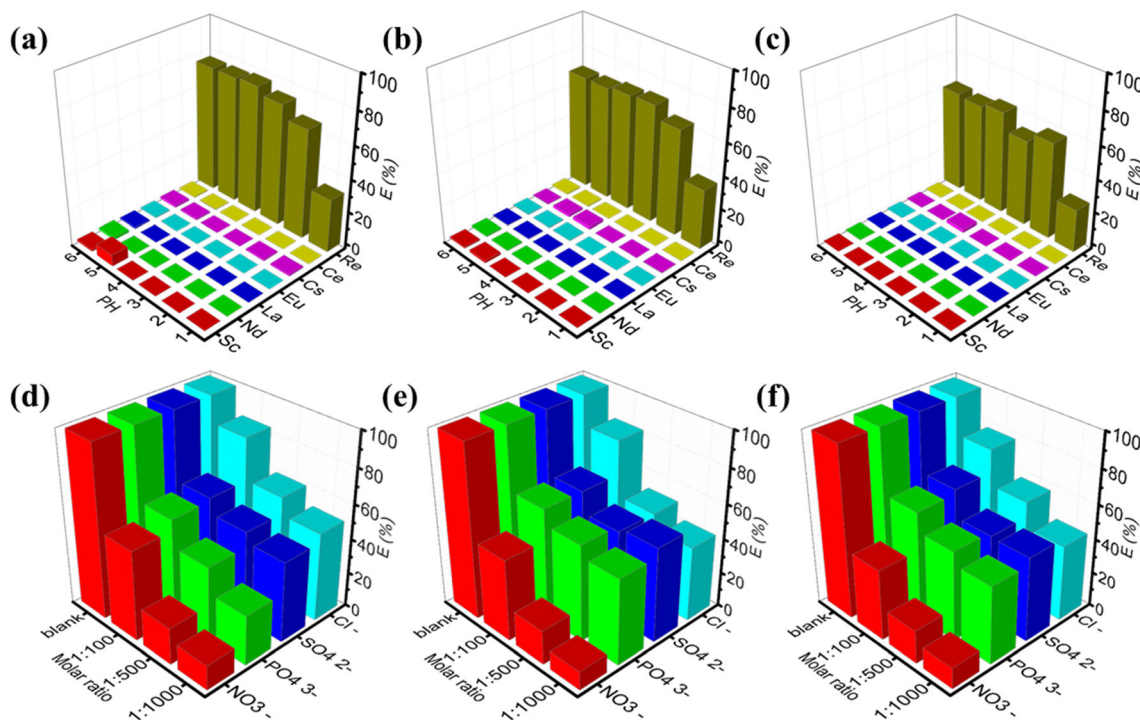


Fig. 6 Effect of coexisting cations and anions on the removal efficiency of ReO_4^- onto SVIL-C1 (**a, d**), SVIL-C4 (**b, e**), SVIL-C8 (**c, f**) (The initial concentration of ReO_4^- and other coexisting cations were 20 ppm.)

positively charged imidazole ring and the negatively charged ReO_4^- (Mu et al.).

Many reports proved that ReO_4^- was difficult to be complexed, and their adsorption mechanism was mainly ion exchange (Katayev et al. 2009; Lou et al. 2019; Ding et al. 2020). A few researchers found that ReO_4^- was reduced to ReO_2 during the adsorption process (Sheng et al. 2016; Wang et al. 2019). Besides, the adsorption mechanism of imidazolium-based adsorbents was mainly ion exchange (Han et al. 2018; Lou et al. 2019). In this work, FT-IR and XPS results indicated that ion exchange occurred during adsorption without a redox reaction. Therefore, we think that the adsorption mechanism of ReO_4^- by SVIL-Cn was ion exchange. To further determine the ion exchange mechanism, SVIL-Cn was immersed into ReO_4^- solutions with different

concentrations ranging from 10 to 120 mg L^{-1} . The released Cl^- was measured and compared to the amount of the ReO_4^- removed from solution. As shown in Fig. S4a, the concentration of released Cl^- increased with the concentration of removed ReO_4^- . The number of moles of released Cl^- was slightly greater than the moles of ReO_4^- removed due to chlorine hydrolysis of the unreacted VBC (Fig. S5). To prove this point, SVIL-Cn was added to deionized water and shaken for 12 h, and then the released Cl^- was measured (Table S3). After deducting the Cl^- generated by the hydrolysis of SVIL-Cn, the molar ratio of the released Cl^- to the removed ReO_4^- was very close to 1:1. We also measured the conductivity of the solution before and after adsorption, and the results are shown in Fig. S4b. The conductivity of the solution after adsorption was slightly higher than that before

Fig. 7 Removal efficiency of ReO_4^- onto SVIL-Cn after irradiated by β -rays (**a**) and γ -rays (**b**) ($c_0 = 20$ ppm)

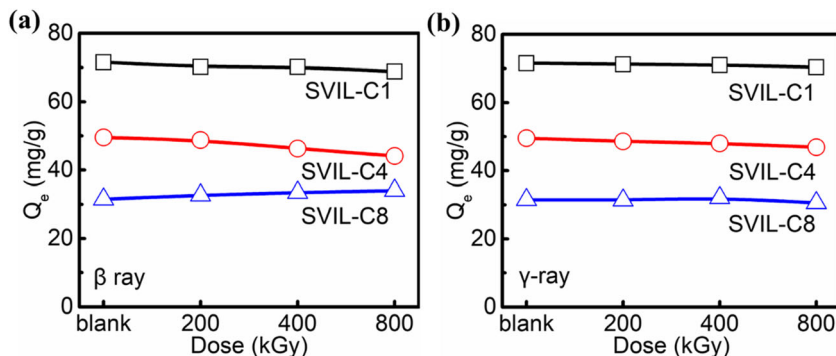
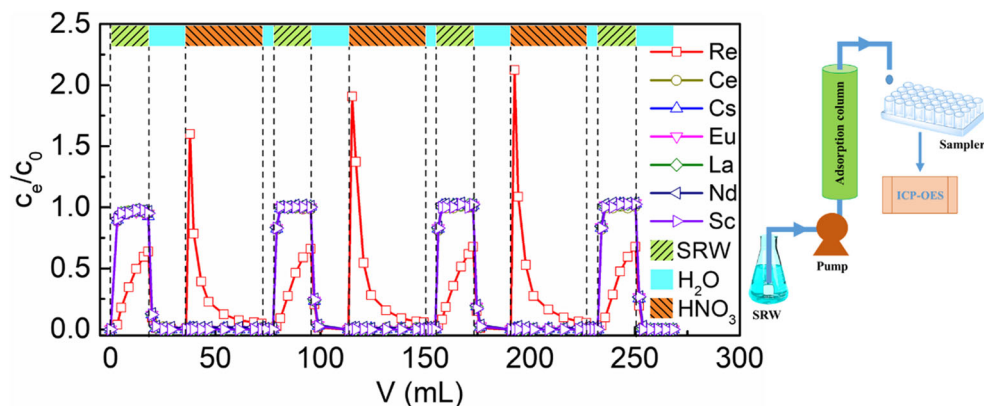


Fig. 8 The column experiment curves of SVIL-C1 for the separation of ReO_4^- from SRW (all cations: 0.1 mmol L^{-1} , HNO_3 : 0.5 mol L^{-1})



adsorption, which was also due to the chlorine hydrolysis of the unreacted VBC. After deducting the conductivity increase due to the hydrolysis of SVIL-Cn (Table S3), the conductivity of the solution before and after adsorption was almost equal.

To summarize, the adsorption mechanism of ReO_4^- by SVIL-C1 was an ion exchange process without a redox reaction in which ReO_4^- replaced Cl^- on SVIL-C1 and combined with SVIL-C1 via electrostatic interactions between ReO_4^- and the imidazole ring.

Conclusions

In conclusion, we reported a novel method for the synthesis of ionic liquid–modified silica-based adsorbents (SVIL-Cn) through radiation grafting. The SVIL-Cn exhibited adsorption capacity of $30.57 \sim 70.62 \text{ mg g}^{-1}$ and the good selectivity in the presence of a large excess of other competing anions. The difference of adsorption performance was mainly determined by the molar content of imidazolium, and the hydrophobicity

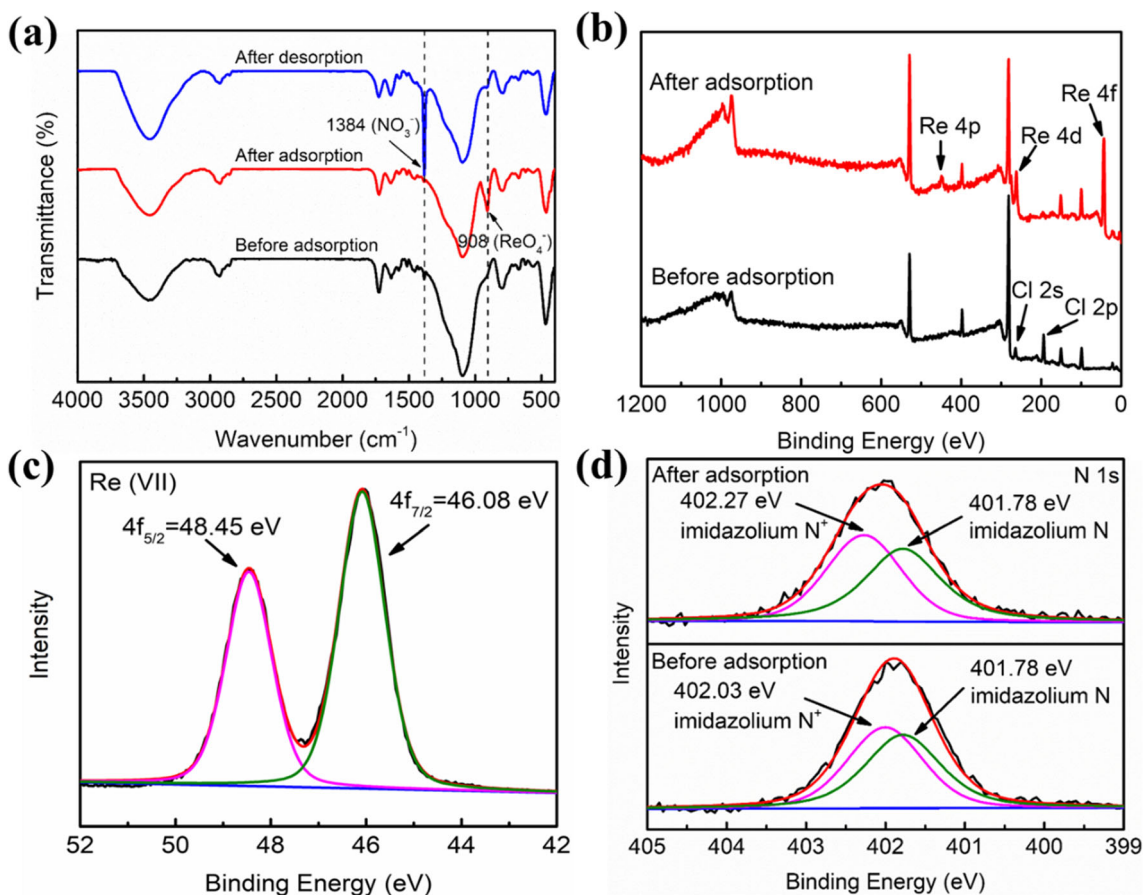


Fig. 9 **a** FT-IR spectra of SVIL-C1 before and after adsorption as well as after desorption. **b** XPS spectra of SVIL-C1 before and after adsorption. **c** Re 4f spectra of SVIL-C1 after adsorption. **d** N 1s spectra of SVIL-C1 before and after adsorption

and steric hindrance also have a synergistic effect. Besides, SVIL-Cn showed excellent resistance toward strong ionizing radiation. The column experiment results of treating SRW proved that SVIL-Cn were able to realize the selective separation of $\text{TcO}_4^-/\text{ReO}_4^-$ from a variety of fission products. In addition, the adsorption mechanism was ion exchange process between Cl^- and ReO_4^- , which confirmed by FT-IR and XPS analysis. These results demonstrated that SVIL-Cn showed a powerful application potential for efficient removal of $\text{TcO}_4^-/\text{ReO}_4^-$ from radioactive wastewater.

Supplementary Information The online version contains supplementary material available at <https://doi.org/10.1007/s11356-020-12078-z>.

Acknowledgments The authors would like to thank the Analytical and Testing Center of Huazhong University of Science and Technology for providing the facilities to fulfill the experimental measurements.

Authors' contributions Kangjun Xie: Conceptualization, data curation, writing - original draft, and methodology. Zhen Dong: Formal analysis, investigation, and funding acquisition. Long Zhao: Writing - review and editing, funding acquisition, and supervision. All authors read and approved the final manuscript

Funding This work was supported by the National Natural Science Foundation of China (11875138, 11905070) and the China Postdoctoral Science Foundation (2019M650180, 2020T130222). This work was also supported by a grant from the nuclear energy development program of state administration of science, Technology and Industry for National Defence, PRC.

Data availability All data generated or analyzed during this study are included in this published article and its supplementary information files.

Compliance with ethical standards

Competing interest The authors declare that they have no competing interests.

Ethics approval and consent to participate Not applicable.

Consent for publication Not applicable.

References

- Banerjee D, Kim D, Michael J (2016) Removal of TcO_4^- ions from solution: materials and future outlook. *Chem Soc Rev* 45:2724–2739. <https://doi.org/10.1039/C5CS00330J>
- Chen L, Chen Y, Wang X, Wei Y, He L, Tang F (2017) A novel silica-based anion exchange resin used for removing uranium from drinking water. *J Radioanal Nucl Chem* 314(3):2569–2578. <https://doi.org/10.1007/s10967-017-5611-5>
- Ding M, Chen L, Xu Y, Chen B, Ding J, Wu R, Huang C, He Y, Jin Y, Xia C (2020) Efficient capture of Tc/Re(VII, IV) by a viologen-based organic polymer containing tetraaza macrocycles. *Chem Eng J* 380:122581. <https://doi.org/10.1016/j.cej.2019.122581>
- Dong Z, Zhao L (2018) Surface modification of cellulose microsphere with imidazolium-based ionic liquid as adsorbent: effect of anion variation on adsorption ability towards Au(III). *Cellulose* 25:2205–2216. <https://doi.org/10.1007/s10570-018-1735-1>
- Dong Z, Liu J, Yuan W, Yi Y, Zhao L (2016) Recovery of Au(III) by radiation synthesized aminomethyl pyridine functionalized adsorbents based on cellulose. *Chem Eng J* 283:504–513. <https://doi.org/10.1016/j.cej.2015.07.011>
- Dong Z, Yuan W, Li Y, Hua R, Zhao L (2019) Radiation synthesis of crown ether functionalized microcrystalline cellulose as bifunctional adsorbent: a preliminary investigation on its application for removal of ReO_4^- as analogue for TcO_4^- . *Radiat Phys Chem* 159:147–153. <https://doi.org/10.1016/j.radphyschem.2019.02.054>
- Favre-Réguillon A, Draye M, Cote G, Czerwinsky KR (2019) Insights in uranium extraction from spent nuclear fuels using dicyclohexano-18-crown-6-Fate of rhenium as technetium homolog. *Sep Purif Technol* 209:338–342. <https://doi.org/10.1016/j.seppur.2018.07.034>
- Feng WQ, Lu YH, Chen Y, Lu YW, Yang T (2016) Thermal stability of imidazolium-based ionic liquids investigated by TG and FTIR techniques. *J Therm Anal Calorim* 125(1):143–154. <https://doi.org/10.1007/s10973-016-5267-3>
- Galamboš M, Daňo M, Viglašová E, Daňo M, Viglašová E, Krivosudský L, Roszkopfová O, Novák I, Berek I, Rajec P (2015) Effect of competing anions on pertechnetate adsorption by activated carbon. *J Radioanal Nucl Chem* 304:1219–1224. <https://doi.org/10.1007/s10967-015-3953-4>
- Han D, Li X, Cui Y, Yang X, Chen X, Xu L, Peng J, Li J, Zhai M (2018) Polymeric ionic liquid gels composed of hydrophilic and hydrophobic units for high adsorption selectivity of perchlorate. *RSC Adv* 8: 9311–9319. <https://doi.org/10.1039/C8RA00838H>
- Herman H, Slade RCT, Varcoe JR (2003) The radiation-grafting of vinylbenzyl chloride onto poly(hexafluoropropylene-co-tetrafluoroethylene) films with subsequent conversion to alkaline anion-exchange membranes: optimisation of the experimental conditions and characterisation. *J Membr Sci* 218(1/2):147–163. [https://doi.org/10.1016/S0376-7388\(03\)00167-4](https://doi.org/10.1016/S0376-7388(03)00167-4)
- Jie L, Xing D, Lin Z, Chao X, Duo Z, Silver MA et al (2018) $^{99}\text{TcO}_4^-$ remediation by a cationic polymeric network. *Nat Commun* 9(1): 3007. <https://doi.org/10.1038/s41467-018-05380-5>
- Katayev EA, Kolesnikov GV, Sessler JL (2009) Molecular recognition of pertechnetate and perchlorate. *Chem Soc Rev* 38(6):1572–1586. <https://doi.org/10.1039/b806468g>
- Lee MS, Um W, Wang G, Kruger AA, Lukens WW, Rousseau R, Glezakou VA (2016) Impeding $^{99}\text{Tc(IV)}$ mobility in novel waste forms. *Nat Commun* 7:12067. <https://doi.org/10.1038/ncomms12067>
- Lin Z, Xiao C, Dai X et al (2017) Exceptional perchlorate/pertechnetate uptake and subsequent immobilization by a low-dimensional cationic coordination polymer: overcoming the Hofmeister bias selectivity. *Environ Sci Technol Lett* 4:316–322. <https://doi.org/10.1021/acs.estlett.7b00165>
- Liu ZW, Han BH (2019) Evaluation of an imidazolium-based porous organic polymer as radioactive waste scavenger. *Environ Sci Technol* 54(1):216–224. <https://doi.org/10.1021/acs.est.9b05308>
- Lou Z, Huang M, Cui J, Wu S, Xing S, Zhou P, Shan W, Xiong Y (2019) Copolymers of vinylimidazolium-based ionic liquids and divinylbenzene for adsorption of TcO_4^- or ReO_4^- . *Hydrometallurgy* 190:105147. <https://doi.org/10.1016/j.hydromet.2019.105147>
- Mahmoud ME, Al-Bishri HM (2011) Supported hydrophobic ionic liquid on nano-silica for adsorption of lead. *Chem Eng J* 166:157–167. <https://doi.org/10.1016/j.cej.2010.10.046>
- Morin-Crini N, Fourmentin M, Fourmentin S, Torri G, Crini G (2018) Synthesis of silica materials containing cyclodextrin and their applications in wastewater treatment. *Environ Chem Lett* 17:683–696. <https://doi.org/10.1007/s10311-018-00818-0>

- Pepper SE, Ogden MD (2013) Perrhenate extraction studies by Cyphos 101-IL; screening for implementation in technetium removal. *Sep Purif Technol* 118:847–852. <https://doi.org/10.1016/j.seppur.2013.08.029>
- Qian G, Song H, Yao S (2016) Immobilized chiral tropine ionic liquid on silica gel as adsorbent for separation of metal ions and racemic amino acids. *J Chromatogr A* 1429:127–133. <https://doi.org/10.1016/j.chroma.2015.11.083>
- Sheng G, Tang Y, Linghu W, Wang L, Li J, Li H, Wang X, Huang Y (2016) Enhanced immobilization of ReO_4^- by nanoscale zerovalent iron supported on layered double hydroxide via an advanced XAFS approach: implications for TcO_4^- sequestration. *Appl Catal B Environ* 192:268–276. <https://doi.org/10.1016/j.apcatb.2016.04.001>
- Sheng D, Zhu L, Xu C, Xiao C, Wang S (2017) Efficient and selective uptake of TcO_4^- by a cationic metal-organic framework material with open Ag^+ sites. *Environ Sci Technol* 51:3471–3479. <https://doi.org/10.1021/acs.est.7b00339>
- Sheng D, Zhu L, Dai X, Xu C, Li P, Pearce C, Xiao C, Chen J, Zhou R, Duan T, Farha O, Chai Z, Wang S (2019) Successful decontamination of $^{99}\text{TcO}_4^-$ in groundwater at legacy nuclear sites by a cationic metal-organic framework with hydrophobic pockets. *Angew Chem Int Ed Engl* 58:4968–4972. <https://doi.org/10.1002/anie.201814640>
- Shi K, Hou X, Roos P, Wu W (2012) Determination of technetium-99 in environmental samples: a review. *Anal Chim Acta* 709:1–20. <https://doi.org/10.1016/j.aca.2011.10.020>
- Ting TM, Nasef MM (2017) Modification of polyethylene-polypropylene fibers by emulsion and solvent radiation grafting systems for boron removal. *Fiber Polym* 18(6):1048–1055. <https://doi.org/10.1007/s12221-017-6840-5>
- Ting TM, Nasef MM, Hashim K (2015) Modification of nylon-6 fibres by radiation-induced graft polymerisation of vinylbenzyl chloride. *Radiat Phys Chem* 109:54–62. <https://doi.org/10.1016/j.radphyschem.2014.12.010>
- Wang L, Song H, Yuan LY, Li ZJ, Zhang P, Gibson JK, Zheng LR, Wang HQ, Chai ZF, Shi WQ (2019) Effective removal of anionic Re(VII) by surface-modified $\text{Ti}_2\text{CTx MXene}$ nanocomposites: implications for Tc(VII) sequestration. *Environ Sci Technol* 53(7):3739–3747. <https://doi.org/10.1021/acs.est.8b07083>
- Wang Y, Xie M, Lan J, Yuan L, Yu J, Li J, Peng J, Chai Z, Gibson J, Zhai M, Shi W (2020) Radiation controllable synthesis of robust covalent organic framework conjugates for efficient dynamic column extraction of $^{99}\text{TcO}_4^-$. *Chem* 6:2796–2809. <https://doi.org/10.1016/j.chempr.2020.08.005>
- Wang Y, Han D, Zhong S, Li X, Zhai M (2021) Quaternary phosphonium modified cellulose microsphere adsorbent for ^{99}Tc decontamination with ultra-high selectivity. *J Hazard Mater* 401:123354. <https://doi.org/10.1016/j.jhazmat.2020.123354>
- Xiao P, Han D, Zhai M, Xu L, Li H (2016) Comparison with adsorption of Re(VII) by two different γ -radiation synthesized silica-grafting of vinylimidazole/4-vinylpyridine adsorbents. *J Hazard Mater* 324:711–723. <https://doi.org/10.1016/j.jhazmat.2016.11.045>
- Xie K, Dong Z, Wang Y, Qi W, Zhao L (2019) Facile preparation of EVOH-based amphoteric ion exchange membrane using radiation grafting technique: a preliminary investigation on its application for vanadium redox flow battery. *Polymers* 11(5):843. <https://doi.org/10.3390/polym11050843>
- Xingxiao L, Dong H, Taotao G, Jing P, Ling X, Maolin Z (2018) Quaternary phosphonium modified hierarchically macro/mesoporous silica for fast removal of perrhenate. *Ind Eng Chem Res* 57:13511–13518. <https://doi.org/10.1021/acs.iecr.8b03306>
- Xu H, Fang J, Guo M, Lu X, Wei X, Tu S (2010) Novel anion exchange membrane based on copolymer of methyl methacrylate, vinylbenzyl chloride and ethyl acrylate for alkaline fuel cells. *J Membr Sci* 354(1–2):206–211. <https://doi.org/10.1016/j.memsci.2010.02.028>
- Xu L, Sun J, Zhao L (2011) Co-grafting of acrylamide and vinyl imidazole onto EB pre-irradiated silanized silica gel. *Radiat Phys Chem* 80(11):1268–1274. <https://doi.org/10.1016/j.radphyschem.2011.03.024>
- Yang J, Shi K, Gao X, Hou X, Shi W (2019) Hexadecylpyridinium (HDPy) modified bentonite for efficient and selective removal of ^{99}Tc from wastewater. *Chem Eng J* 382:122894. <https://doi.org/10.1016/j.cej.2019.122894>
- Yu P, Wang S, Alekseev VE et al (2010) Technetium-99 MAS NMR spectroscopy of a cationic framework material that traps TcO_4^- ions. *Angew Chem* 49:5975–5977. <https://doi.org/10.1002/anie.201002646>
- Zhao L, Sun J, Zhao Y, Xu L, Zhai M (2011) Removal of hazardous metal ions from wastewater by radiation synthesized silica-graft-dimethylaminoethyl methacrylate adsorbent. *Chem Eng J* 170:162–169. <https://doi.org/10.1016/j.cej.2011.03.047>
- Zhao Z, Sun X, Dong Y, Wang Y (2016) Synergistic effect of acid-base coupling bifunctional ionic liquids in impregnated resin for rare earth adsorption. *ACS Sustain Chem Eng* 4:616–624. <https://doi.org/10.1021/acssuschemeng.5b01253>
- Zsabka P, Van Hecke K, Adriaensen L, Wilden A, Modolo G, Verwerf M et al (2019) Solvent extraction of Am(III) , Cm(III) , and Ln(III) ions from simulated highly active raffinate solutions by TODGA diluted in Aliquat-336 nitrate ionic liquid. *Solvent Extr Ion Exc* 36:519–541. <https://doi.org/10.1080/07366299.2018.1545288>
- Zu J, Ye M, Wang P et al (2016a) Design of a strong-base anion exchanger and its adsorption and elution behavior for rhenium(VII). *RSC Adv* 6:18868–18873. <https://doi.org/10.1039/c5ra25313f>
- Zu J, Liu R, Zhang J, Tang F, He L (2016b) Adsorption of Re and Tc-99 by means of radiation-grafted weak basic anion exchange resin. *J Radioanal Nucl Chem* 310:229–237. <https://doi.org/10.1007/s10967-016-4819-0>

Publisher's note Springer Nature remains neutral with regard to jurisdictional claims in published maps and institutional affiliations.